# Marine diatoms record Late Holocene regime shifts in the Pikialasorsuaq ecosystem

Audrey Limoges, Sofia Ribeiro, Nicolas van Nieuwenhove, Rebecca Jackson, Stephen Juggins, Xavier Crosta, Kaarina Weckström

Received: 21 May 2023 | Revised: 10 August 2023 | Accepted: 12 September 2023

DOI: 10.1111/gcb.16958

Global Change Biology WILEY

RESEARCH ARTICLE

# Marine diatoms record Late Holocene regime shifts in the Pikialasorsuaq ecosystem

Audrey Limoges[1] | Sofia Ribeiro[2] | Nicolas Van Nieuwenhove[1] | Rebecca Jackson[2,3] | Stephen Juggins[4] | Xavier Crosta[5] | Kaarina Weckström[6]

[1]Department of Earth Sciences, University of New Brunswick, Fredericton, New Brunswick, Canada

[2]Department of Glaciology and Climate, Geological Survey of Denmark and Greenland, Copenhagen, Denmark

[3]Globe Institute, Copenhagen University, Copenhagen, Denmark

[4]School of Geography, Politics and Sociology, Newcastle University, Newcastle upon Tyne, UK

[5]CNRS, EPHE, UMR 5805 EPOC, Université de Bordeaux, Pessac Cedex, France

[6]Ecosystems and Environment Research Programme (ECRU), University of Helsinki, Helsinki, Finland

**Correspondence**
Audrey Limoges, Department of Earth Sciences, University of New Brunswick, 2 Bailey Drive, Fredericton, NB E3B 5A3, Canada.
Email: alimoges@unb.ca

**Funding information**
Arctic Avenue; ArcticNet, Grant/Award Number: 206; Independent Research Fund, Denmark, Grant/Award Number: 9064-00039B; Natural Sciences and Engineering Research Council of Canada, Grant/Award Number: 2018-03984

## Abstract

The Pikialasorsuaq (North Water polynya) is an area of local and global cultural and ecological significance. However, over the last decades, the region has been subject to rapid warming, and in some recent years, the seasonal ice arch that has historically defined the polynya's northern boundary has failed to form. Both factors are deemed to alter the polynya's ecosystem functioning. To understand how climate-induced changes to the Pikialasorsuaq impact the basis of the marine food web, we explored diatom community-level responses to changing conditions, from a sediment core spanning the last 3800 years. Four metrics were used: total diatom concentrations, taxonomic composition, mean size, and diversity. Generalized additive model statistics highlight significant changes at ca. 2400, 2050, 1550, 1200, and 130 cal years BP, all coeval with known transitions between colder and warmer intervals of the Late Holocene, and regime shifts in the Pikialasorsuaq. Notably, a weaker/contracted polynya during the Roman Warm Period and Medieval Climate Anomaly caused the diatom community to reorganize via shifts in species composition, with the presence of larger taxa but lower diversity, and significantly reduced export production. This study underlines the high sensitivity of primary producers to changes in the polynya dynamics and illustrates that the strong pulse of early spring cryopelagic diatoms that makes the Pikialasorsuaq exceptionally productive may be jeopardized by rapid warming and associated Nares Strait ice arch destabilization. Future alterations to the phenology of primary producers may disproportionately impact higher trophic levels and keystone species in this region, with implications for Indigenous Peoples and global diversity.

KEYWORDS
Arctic, climate change, diatom phenology, ecosystem functioning, marine sediment, North Water polynya, northern Baffin Bay, primary production

## 1 | INTRODUCTION

Climate warming and polar amplification threaten the formation and maintenance of Arctic polynyas, which are rapidly responding to a shrinking cryosphere. The Pikialasorsuaq, or North Water (NOW) polynya, located in northern Baffin Bay between Ellesmere Island (Nunavut) and Northwest Greenland (Figure 1), develops south of an ice arch that consolidates across the narrow head of Smith Sound, Nares Strait. Historically, the ice arch blocks the inflow of ice from the Lincoln Sea and Kane Basin and promotes continuous mechanical removal of newly formed sea ice within the NOW by ocean currents and the polar easterlies channeled through the strait. Near the Northwest Greenland coast, sensible heat is also brought near the surface by upwelling of the relatively warm West Greenland Current, which further dampens sea-ice growth (Melling et al., 2001; Mundy & Barber, 2001; Steffen, 1985) and can contribute to polynya formation even in the absence of an ice arch (Moore et al., 2023). In addition to these processes, strong tide-induced movement of ice contributes to open waters over the short term (Vincent & Marsden, 2008). The NOW has the largest biological production per unit area of any waters in the Arctic (Barber & Massom, 2007) and is a pivotal site for resource and energy transfer to regional ecosystems since at least ca. 4400 years BP (Davidson et al., 2018; Mosbech et al., 2018; Ribeiro et al., 2021; Tremblay & Smith, 2007). However, starting in the 1990s, instability and earlier seasonal collapse of the Nares Strait ice arch compared with previous decades has led to increased variability in the seasonal duration, extent and spatial configuration of the NOW (e.g., Preußer et al., 2015; Vincent, 2019, 2020), with implications for the future of this important ecosystem.

The abundance and taxonomic composition of unicellular primary producers, forming the basis of the marine food web, are controlled by a suite of interacting parameters such as temperature, sea ice, availability of light and nutrients (nitrate, phosphorus, silicate, and trace elements), processes affecting water column stratification and mixing, and top-down regulation. In the NOW, diatoms play a critical functional role as the dominant pelagic primary producers (Lovejoy et al., 2002; Tremblay et al., 2002), fostered by the early exposure to light, the input of silicate-rich modified Pacific waters (Coachman & Aargaard, 1988;

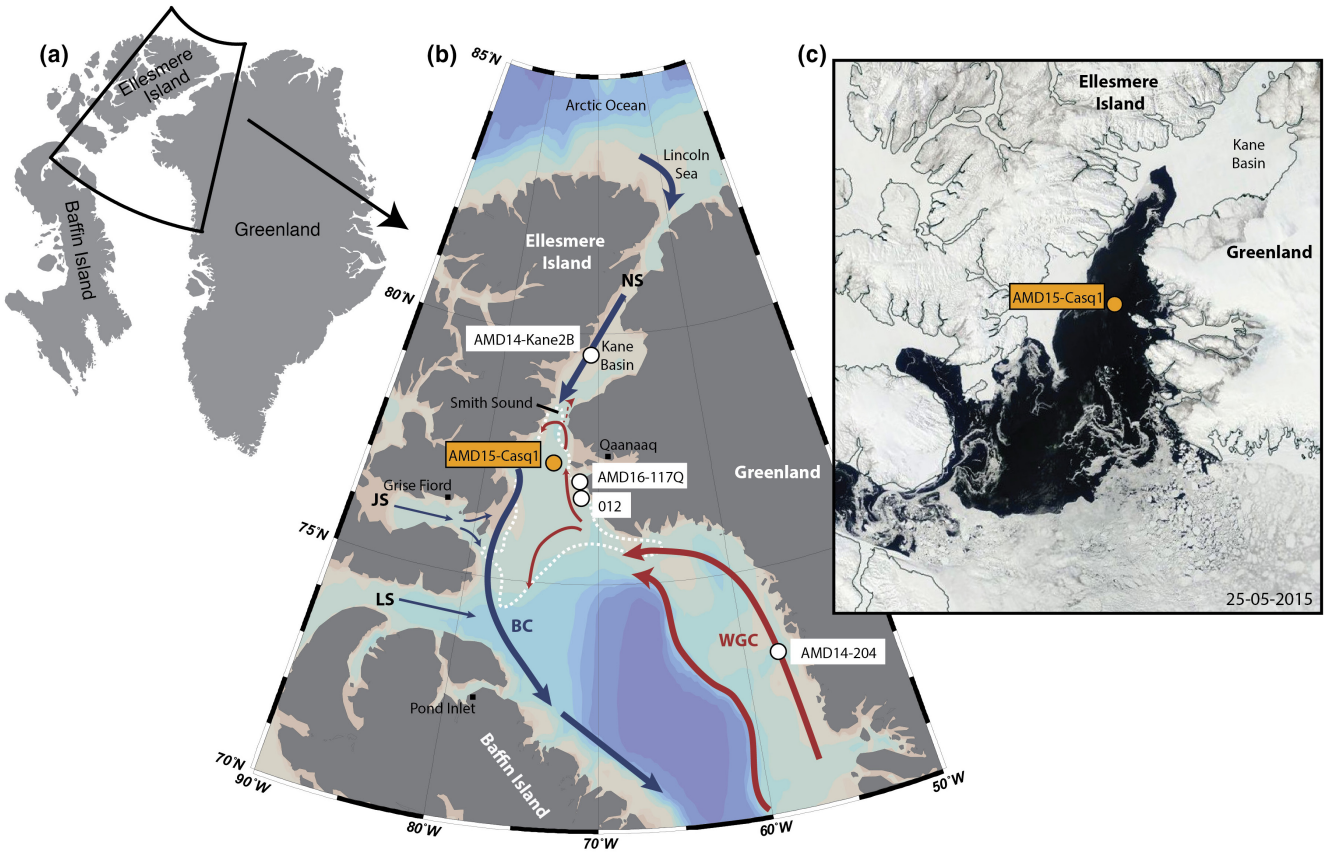


FIGURE 1 Study area and satellite image of the Pikialasorsuaq. (a) Geographical location of the study area, (b) map showing the surface/subsurface circulation in northern Baffin Bay (red arrows for relatively warm water masses and blue arrows for cold water masses), approximate extent of the NOW (white dashed line), and locations of the sampling site from which core AMD15-Casq1 was retrieved (yellow circle; this study) and sampling sites from which cores AMD14-Kane2B (Caron et al., 2019; Georgiadis et al., 2020), AMD14-204C (Limoges et al., 2020), AMD16-117Q (Jackson et al., 2021) and 012 (Knudsen et al., 2008) were retrieved, and (c) NASA EOSDIS satellite image showing the configuration of the Pikialasorsuaq in spring 2015 (year of core collection), with a well-consolidated Nares Strait ice arch. BC, Baffin Island Current; JS, Jones Sound; LS, Lancaster Sound; NS, Nares Strait; WGC, West Greenland Current.

Münchow et al., 2006), and a high mixing regime (Michel et al., 2015). Diatoms play a key role in sustaining a productive food web and are one of the main vectors of carbon export to the deep ocean and sediments (e.g., Tréguer et al., 2018). Yet, we know little about the long-term interactions of diatom production and community structure with ocean conditions in the NOW. This limits our capacity to project their future responses to a changing environment and develop prognostic models of how changes will be propagated through the entire food web.

Ecosystem regime shifts are sudden and persistent changes in the structure and dynamics of a system that result from crossing critical environmental thresholds and which encompass multiple physicochemical and biological variables, including keystone species (e.g., Dakos et al., 2019; Möllmann et al., 2015). These abrupt transitions between alternative ecological regimes show that natural systems are not always responding linearly or predictably. Better understanding of multilevel responses to environmental drivers (i.e., from microbial organisms to higher trophic levels) and the ability to identify regional shifts is therefore relevant to management and conservation efforts.

Marine sediment records can provide insight into how a biota responds to ecosystem regime shifts occurring beyond the instrumental era. Because diatoms represent a diverse spectrum of ecological optima and tolerances and respond sensitively to environmental changes, their amorphous biogenic silica ($bSiO_2$) skeletons (frustules and resting stages) preserved in sediment are commonly used as paleoenvironmental indicators. Diatoms also display a broad range of size and silicification levels and show a continuous range of growth strategies, which affect crucial ecological processes such as the energy transfer to higher trophic levels, biogeochemical cycling, light harvesting, cell growth, and sinking rates (e.g., Behrenfeld et al., 2021; Finkel et al., 2004; Ryabov et al., 2021; and references therein). Although paleoenvironmental studies most often report diatom counts irrespective of cell size, diatoms appear to have scale-dependent responses to environmental constraints, which can in turn affect ecosystem structure and function (Finkel et al., 2005; Snoeijs et al., 2002).

Here, we investigate multidecadal changes in community-level responses of diatoms using a well-dated sediment record from the NOW. We reconstructed diatom abundance, cell size, diversity, and taxonomic composition over the last ca. 3800 years. While biogenic silica dissolution is strongly governed by silicic acid availability, pH, and temperature (Kamatani & Riley, 1979; Hurd & Birdwhistell, 1983; Ragueneau et al., 2000; Taucher et al., 2022), it has been shown to be relatively limited in the near-freezing waters of the NOW (Michel et al., 2002; Tremblay et al., 2002). Furthermore, this work is based on the analysis of a 5.43 m long marine sediment core that has previously been the subject of paleoenvironmental studies (Jackson et al., 2021; Koerner et al., 2021; Ribeiro et al., 2021), offering an ideal framework to understand the impacts of climate-forced changes in polynya dynamics on diatom production and composition and discuss possible implications for future ecosystem functioning.

## 2 | OCEAN CIRCULATION AND SEA-ICE CONDITIONS

Along the Greenland coast, a branch of the subsurface West Greenland Current flows north and has been tracked up the Greenland side of Nares Strait almost to the Lincoln Sea (Münchow et al., 2007), supplying relatively warm, saline (>1°C, >33.9 psu; Münchow et al., 2015), and nitrate-rich (~14.5 μmol $kg^{-1}$; Tremblay et al., 2002) waters to the NOW (Figure 1b). The West Greenland Current is composed of a mixture of water carried by the East Greenland Current and water derived from the Irminger Current. This current upwells in the eastern sector of the NOW to the base of the turbulent surface layer, and a flow component also veers west to feed into the south-flowing Baffin Island Current (Dumont et al., 2010; Melling et al., 2001). Colder and fresher (<−0.4°C; <33.5 psu; Münchow et al., 2015) silicate- and phosphate-rich (up to 18 and 1.1 μmol $kg^{-1}$, respectively; Burgers et al., 2023) Pacific-derived Arctic waters have been reported to enter the NOW from the north through Nares Strait (sill depth of 220 m; Lehmann et al., 2022; Tremblay et al., 2002) driven by strong and persistent northerly winds and a sea-level difference between the Lincoln Sea and northern Baffin Bay. However, it is worth noting that the water mass assembly and nutrient content entering Nares Strait from the Lincoln Sea vary under different atmospheric forcing patterns (i.e., Arctic Oscillation modes), with increased contribution of the fresher and nutrient-depleted (nitrate concentrations below 1 μM during winter; Brown et al., 2020) surface waters of the Canada basin during positive phases of the Arctic Oscillation and increased contribution of the comparatively nutrient-rich waters (nitrate concentrations up to 3.5 μmol $kg^{-1}$) of the Siberian shelves during neutral/negative phases of the Arctic Oscillation (Burgers et al., 2023). Pacific-derived Arctic waters that are modified by meltwater input during their transit through the Canadian Arctic Archipelago also enter the NOW from the west through the shallower Lancaster (sill depth 125 m) and Jones (sill depth 190 m) sounds (Lehmann et al., 2022; Ren et al., 2022).

Although sensible heat is also responsible for sea-ice melt in its eastern sector, especially during the autumn (Melling et al., 2001), the Pikialasorsuaq primarily exists through a balance between sea-ice formation and drift and is as such classified as a latent heat polynya. Sea ice is blown away southward from the Nares Strait ice arch, and this stimulates new sea-ice growth (i.e., the sea-ice factory). When the ice arch is present, the polynya recurrently opens from March or early April and expands southward of Smith Sound (Barber & Massom, 2007). In June or July, when the ice arch usually breaks, the area transitions to a marginal ice zone (MIZ; Vincent, 2019). By contrast, when the ice arch does not form, such as during the 2006/2007 winter, ice is advected year-round through Nares Strait from north to south (Münchow et al., 2007) and the polynya fails to form until late May. The NOW is thus tightly influenced by changes in atmospheric temperature and circulation, which impact sea-ice dynamics and ocean circulation (e.g., Ren et al., 2022) and can push the ecosystem into different functioning modes. Understanding the

evolution of the NOW through the Late Holocene can thus provide context to assess the future trajectory of this ecosystem.

## 3 | MATERIALS AND METHODS

A Calypso Square gravity core AMD15-Casq1 (543 cm) and corresponding box core (40 cm) were collected in 2015 from the central north NOW (77°15.035′ N, 74°25.500′ W, 692 m water depth; Figure 1) during the ArcticNet Leg 4a, onboard the Canadian Coast Guard Ship *Amundsen*.

### 3.1 | Age model

The core chronology is based on 11 accelerator mass spectrometry dates on mollusk shells from the Calypso core and $^{210}$Pb and $^{137}$Cs measurements on 20 samples from the box core (see Jackson et al., 2021 for more details). Here, all radiocarbon dates were calibrated using the latest marine calibration curve (Marine20; Heaton et al., 2020; Tables S1 and S2). In Jackson et al. (2021), and using the Marine13 calibration curve, a local reservoir correction of 140 ± 60 years was applied based on measurements from a live marine mollusk specimen collected from the NOW before the mid-1950s (McNeely & Brennan, 2005). Using the Marine20 calibration curve, this specimen now yields a reservoir offset of −4 ± 60 years. In line with this reduced reservoir offset for the Marine 20 (vs. Marine13) calibration curve, and owing to the lack of a regional ΔR term for the polynya (Pieńkowski et al., 2023), no additional reservoir age correction (i.e., $\Delta R = 0$) was applied. A mixed age-depth model was constructed using the bacon package in R (Blaauw & Christen, 2011). Accordingly, the composite core covers the last ca. 3800 cal years BP. We note that the new calibration only resulted in negligible changes compared with the age model presented in Jackson et al. (2021).

### 3.2 | Diatom analysis

Sediment samples for diatom analysis were prepared following the protocol described in Crosta et al. (2020). Approximately 0.3 g of dry sediment was treated with an oxidative solution composed of hydrogen peroxide ($H_2O_2$), distilled water and tetrasodium pyrophosphate (decahydrate, $Na_4O_7P_2$-$10H_2O$) in a warm bath (ca. 65°C) for several hours, until the reaction ceased. The residue was then rinsed repeatedly with distilled water by centrifugation (7 min at 1200 rpm). Hydrochloric acid (HCl, 30%) was used to remove the carbonate content. The residue was again rinsed several times until neutral pH, and microscopy slides were mounted in Naphrax©.

In each sample, ca. 300 diatom valves were identified to the lowest taxonomic level possible (Table S3). Resting spores of *Chaetoceros* were counted, but not included in the relative abundance calculations. Census counts were done using a light microscope (Olympus BX53, UNB) with dark field, phase contrast optics and oil immersion, at 1000× magnification. We followed the counting rules presented in Crosta and Koç (2007): Specimens were counted when at least half of the valve was observed, with the exception of *Rhizosolenia* and *Thalassiothrix* taxa that were only counted when the spine-like proboscis or appendix was visible, respectively. Diatoms were analyzed at a 1–10 cm sampling interval, which corresponds to an effective age resolution ranging from ca. 3 to 64 years (mean: 31 years). Absolute abundances are reported in valves per g of dry sediment. Fluxes were calculated by combining diatom concentrations (valves $g^{-1}$) with mass accumulation rates ($g\,cm^{-2}\,year^{-1}$).

### 3.3 | Indicators of taxonomic composition shifts

Principal component (PC) analysis based on a variance–covariance matrix was used to extract the dominant modes of variability in the diatom assemblages (log-transformed percentages excluding *Chaetoceros* resting spores and unidentified diatoms) and define assemblage zones. The analysis was computed using Past 4.10 (Hammer et al., 2001).

Q-mode factor analysis (i.e., relationship among objects; Imbrie & Kipp, 1971) was applied to synthesize temporal compositional changes in the diatom assemblages using eight common water mass signatures, or *factors* (Oksman et al., 2017, 2019). These factors were defined based on the modern surface sediment distribution of diatoms and associated hydrographic conditions in the northern North Atlantic calibration dataset. Q-mode analysis was used to distinguish combinations of co-varying diatom taxa and to identify ecological shifts within the NOW through time.

To assess changes in species diversity and compare downcore communities, we calculated Hill diversity (Hill, 1973), which includes modified versions of the Shannon and Simpson indices (Roswell et al., 2021; Text S1). We note that, when applied to subfossil assemblages, the indices are not representative of the true diversity of the communities (e.g., taphonomic processes, species defined on morphologic grounds). In spite of their limitations, the indices can provide valuable insights into first-order patterns of diversity across time.

### 3.4 | Diatom mean size

The planar dimensions of each dominant taxon were measured at 1000× magnification on permanent slides, using oil immersion, and an eyepiece reticle that was calibrated to a micrometric slide using the Leica Application Suite version 3.3.0. We assumed an uncertainty of ±0.5 µm on the planar measurements. Specimens were measured from each of the main assemblage zones determined in Section 3.3 (Table S4). For pennate diatoms, the apical and transapical axes were measured, and for centric diatoms, the diameter of the cell was measured. In each assemblage zone, between 11 and 162 specimens were measured per species. The average surface areas were calculated from means of measurements for each species and each assemblage zone

using the simplified models presented in Figure S1. For rare species or taxa found only as fragments in the microscopy slides (e.g., *Rhizosolenia*), we used the dimensions reported in the literature (Table S5). To determine whether general patterns of diatom production were associated with changes in the subfossil community size structure, an index based on the relative species abundance and total community mean surface area (all zones combined) was calculated, and values were normalized. Note that this index does not include the resting spores of *Chaetoceros*. To evaluate whether changes in the mean size of diatoms had an impact on the biomass that had accumulated on the seafloor, we multiplied the diatom concentrations by the total diatom surface area for each depth (referred to as "concentration biomass index"). We also calculated a second index, for the Calypso core only, by multiplying the diatom fluxes by the total diatom surface area for each depth (referred to as "flux biomass index"). Since the structural components of the diatom frustules (epitheca, hypotheca, and girdle bands) are often disassembled in the fossil record or during sample preparations, it was not possible to expand the exercise to the third dimension, that is, cellular biovolume calculations. However, the cell volume is strongly correlated to the largest axial dimension (Snoeijs et al., 2002). We note that the indices presented above are not true measures of carbon biomass, which considers the carbon content of a cell as a function of cell volume (e.g., Cornet-Barthaux et al., 2007).

### 3.5 | Data trends and change detection using generalized additive models

Smooth trends were fitted through the downcore data using generalized additive models (GAMs; e.g., Simpson, 2018; Wood, 2017) with the mgcv package (version 1.8-41; Wood, 2017) in the statistical programming environment R (version 4.2.2; R Core Team, 2022) and RStudio (version 2022.07.2; RStudio Team, 2022). GAMs are nonparametric statistical models that use objective automatic smoothness selection methods to estimate trends in data as a function of time. To account for heteroscedasticity (nonconstant variance) in the data due to variations in sedimentation rates, observational weights were used as suggested by Simpson (2018). In order to identify periods of significant change in the trends, the first derivative of the smooth fit through the data and its simultaneous confidence interval was computed using the gratia package (version 0.7.3; Simpson, 2022). GAMs were fitted to the following time series: total diatom concentrations, biomass indices, mean size, diversity indices, and PC1 sample scores on assemblage data.

## 4 | RESULTS

### 4.1 | Diatom assemblages

The diatom assemblages comprise over 40 species belonging to 24 genera (Table S6). The dominant taxa, shown along a seasonal continuum in Figure 2, are as follows: (i) the pack ice species *Actinocyclus curvatulus* (0%–4%), (ii) the pennate early spring bloomers (MIZ species) *Fossulaphycus arcticus* (previously named *Fossula arctica*, 6%–36%), *Fragilariopsis oceanica* (1%–16%), *Fragilariopsis cylindrus* (includes *Fragilariopsis nana*; 1%–38%), *Fragilariopsis reginae-jahniae* (4%–30%), and *Pauliella taeniata* (0%–3%), (iii) the centric late(er) spring bloomers *Thalassiosira bulbosa* (0%–3%), *Thalassiosira nordenskioeldii* (0%–1%), *Thalassiosira antarctica* var. *borealis* (resting spores; 6%–60%), *Porosira glacialis* (2%–16%), and *Thalassiosira hyalina* (0%–6%), and (iv) the summer subsurface group of *Rhizosolenia* species (0%–9%) which includes *Rhizosolenia hebetata* f. *hebetata*, *R. hebetata* f. *semispina*, and unidentifiable species of *Rhizosolenia*.

The leading mode of the principal component (PC1) explains 30% of the variance (Figure 2). *cylindrus* (negative loading of 0.54) and *Rhizosolenia* spp. (positive loading of 0.36) account for a significant portion of the PC1 variance (Table S7). While *F. cylindrus* is an early spring bloomer that thrives in the shallow cold and fresh layer formed by sea-ice melt, *Rhizosolenia* is associated with the late diatom successional patterns and deeper subsurface conditions. PC1 could hence be tentatively related to changes in seasonality and stratification. The second principal component (PC2) explains 10% of the variance. *T. hyalina* and *A. curvatulus* show the strongest positive loading (0.39 and 0.32, respectively) whereas *F. cylindrus* shows the strongest negative loading (−0.29) to PC2. In Baffin Bay, *T. hyalina* is associated with the relatively warm and salty waters of the West Greenland Current and low sea-ice concentrations, whereas *A. curvatulus* is associated with heavy pack ice (Williams, 1986, 1990).

Total diatom concentrations varied 20-fold, ranging between ca. $1\times10^7$ and $2\times10^8$ valves per gram of dry sediment (including *Chaetoceros* resting spores; Figure 2), which translated into fluxes ranging between ca. $9\times10^5$ and $5\times10^7$ valves per $cm^2$ per year. However, since the chronologies of the box and Calypso cores are based on different dating methods ($^{210}Pb$–$^{137}Cs$ activity for the box core and radiocarbon dating for the Calypso core) which are then interpolated by applying statistical methods to develop a continuous depth-age scale for the entire sediment core (composite age model), a skewed bias may exist when calculating mass accumulation rates, which subsequently influence the calculated fluxes. Therefore, to allow comparison between the most recent (box core) and older (Calypso core) parts of the record, we use the concentrations (e.g., valves $g^{-1}$) as comparative units. Even though sediment compaction typically occurs with depth, we note that this record is predominantly composed of silty clay and no major changes in downcore grain-size composition have been observed.

Overall, the small and highly silicified resting spores of *Chaetoceros* represent 18%–56% of the total diatom fluxes. Variation in total concentration and flux is closely mirrored by increased and decreased contribution of *Chaetoceros* resting spores to the total fluxes, which, considering the limited dissolution (see Section 1) and fairly constant and homogenous sedimentation at the core site (Jackson et al., 2021), can be considered a good first-order approximation for total export primary production. Total diatom concentration remained moderately high from ca. 3800 to 2050 cal years BP. A notable decrease in the contribution of the resting spores of

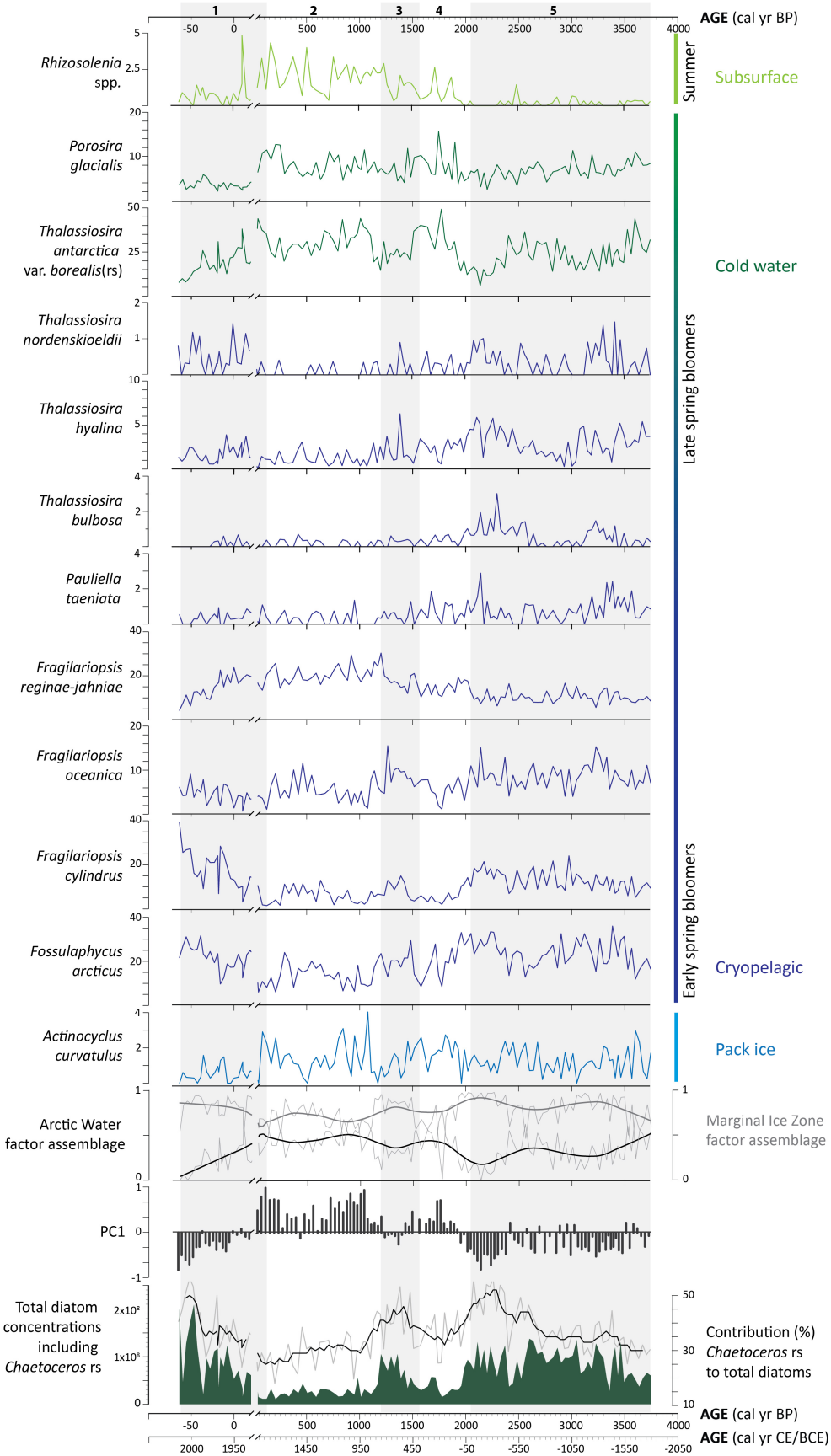


FIGURE 2 Relative abundance (%) of the main diatom taxa (excluding *Chaetoceros* resting spores), contributions of the Arctic water and MIZ factor assemblages defined by Q-mode analysis, PC1, contribution of *Chaetoceros* to the total flux (%), and total diatom flux (includes *Chaetoceros* resting spores; spores and valves dry $g^{-1}$ sediment). The gray boxes delineate the assemblage zones, based on principal component analysis, used for diatom measurements.

*T. antarctica* var. *borealis* and the highest abundance of *T. bulbosa* between 2400 and 2050 cal years BP preceded a drop by two thirds of the total concentration (Figure 2). This decline in export primary production was also accompanied by a *Chaetoceros* fall from peak contribution, a shift from generally negative to positive PC1 scores, and a decline in the Hill–Simpson and Hill–Shannon diversity index values (Figure 4). During the interval of relatively low diatom concentration between ca. 2050 and 1550 cal years BP, the abundances of *Rhizosolenia* spp., *T. antarctica* var. *borealis* (resting spore), and *P. glacialis* increased, whereas the early spring bloomers *F. arcticus*, *F. oceanica*, and *F. cylindrus* decreased. Driven by a short recovery of the early bloomers and *Chaetoceros* resting spores, and a steady increase in *F. reginae-jahniae*, total diatom concentration increased again between ca. 1550 and 1200 cal years BP and this was accompanied by decreased PC1 and increased diversity values. However, from 1200 cal years BP and until ca. 130 cal years BP, concentration was low again with *Chaetoceros* generally contributing <30%. During this same time interval, diversity index values were generally increasing. From ca. 130 cal years BP, diatom concentration increased substantially, steered by the early spring bloomers and an increased contribution of *Chaetoceros*. This trend was accompanied by a return to resolutely negative PC1 scores.

### 4.2 | Q-mode diatom assemblage analysis

The eight factors revealed by Q-mode factor analysis of the surface sediment dataset described in Oksman et al. (2017) explained 91.2% of the total variance in the sedimentary diatom data. This total was dominated by two main assemblages that accounted for 77.4% of the variance: the Arctic water (ArcW) and the MIZ assemblages that showed opposite trends throughout the core (Figure 2). Changes in the contribution of the other Q-mode assemblages are presented in Figure S2. In the modern database, the ArcW assemblage is found between Polar and Atlantic waters including the central-eastern Baffin Bay, whereas the MIZ assemblage dominates in the NOW and near the spring sea-ice edge east of Greenland (Oskman et al., 2017). While the MIZ assemblage dominated over the last 3800 years, the MIZ (ArcW) contribution was generally increased (decreased) from 3800 to 2200 and 1550 to 1200 cal years BP. Increases in the ArcW assemblages were synchronous with increases in the factor of both the Mixed Water Mass (from ca. 0.08 to 0.15) and the Arctic Greenland (from ca. 0 to 0.12) assemblages. In the modern database, the highest contributions of the latter are found in the Greenland Sea, a region influenced by Atlantic-sourced waters. Since ca. 130 cal years BP, a marked decline in the ArcW factor assemblage was accompanied by sustained high contributions of the MIZ assemblage.

### 4.3 | Diatom size

The diatom assemblages preserved in the sediment record are composed of taxa with widely differing shapes and sizes. By far, the largest diatoms are the centric *Coscinodiscus* spp. (mean measured surface area of ca. 33,000 $\mu m^2$) followed by *P. glacialis* (mean measured surface area of ca. 1600 $\mu m^2$), whereas the smallest diatoms are the pennate *F. cylindrus* (mean measured surface area of ca. 45 $\mu m^2$, Figure 3a).

Although *Coscinodiscus* spp. was likely present in all samples and was mostly observed as fragments in the microscopy slides, the large contribution of smaller taxa to the assemblages sometimes led to zero count values for the genus. To assess this sample size effect (detection limit) on our counts, we present the size index excluding and including *Coscinodiscus* spp. (Figure 4). We note that the exclusion or inclusion of *Coscinodiscus* spp. does not influence major index trends but influences the amplitude of the changes. The normalized index values (excluding *Coscinodiscus* spp.) were positive from ca. 3800 cal years BP and declined progressively until ca. 3500 cal years BP, from which point they slightly oscillated around zero. A decline from 2400 to 2050 cal years BP was then followed by one of the largest shifts in mean diatom size. From 2050 cal years BP, values increased substantially to remain dominantly positive until 46 cal years BP, albeit with two intervals of pronounced lower values centered at ca. 1300 and 500 cal years BP. During the last century, a major and rapid decline in the diatom size led to record low values at the top of the core. We note that variations in diatom size structure are significantly correlated with changes in the total diatom concentrations and fluxes, with smaller cells associated with higher concentrations and fluxes ($|r| = .60$, $p < .001$ and $|r| = .73$, $p < .001$, respectively, Figure 3).

The "concentration biomass indices" (Figure 4) suggest that the diatom biomass accumulating on the seafloor declined stepwise from ca. 2700 cal years BP to reach a low value at ca. 1800 cal years BP, but rapidly rose again until ca. 1200 cal years BP. From that time, diatom biomass dropped rapidly to remain low until the start of the twentieth century. Values increased again at ca. 120 cal years BP. The "flux biomass indices" (Figure 4) showed an increasing trend from the bottom of the core until 3000 cal years BP, from which point values decreased until 2200 cal years BP. A low-amplitude increase in the index between 2200 and 2050 cal years BP was followed by a decline. The indices increased again to reach a relatively high value centered at ca. 1300 cal years BP before declining abruptly at ca. 1200 cal years BP. The biomass flux index then remained low for the rest of the Calypso core.

## 5 | DISCUSSION

With a fast growth rate in high-nutrient environments and an affinity for turbulent conditions and the marginal ice edge (Nelson & Tréguer, 1992), diatoms dominate the microplankton communities in the NOW, where they show a strong productivity during the phytoplankton spring bloom (Michel et al., 2002; Tremblay et al., 2006). This bloom can develop as early as May (Lewis et al., 1996; Marchese et al., 2017) and is largely composed of ribbon-forming pennate and Thalassiosiroid taxa. Diatom productivity has been observed to

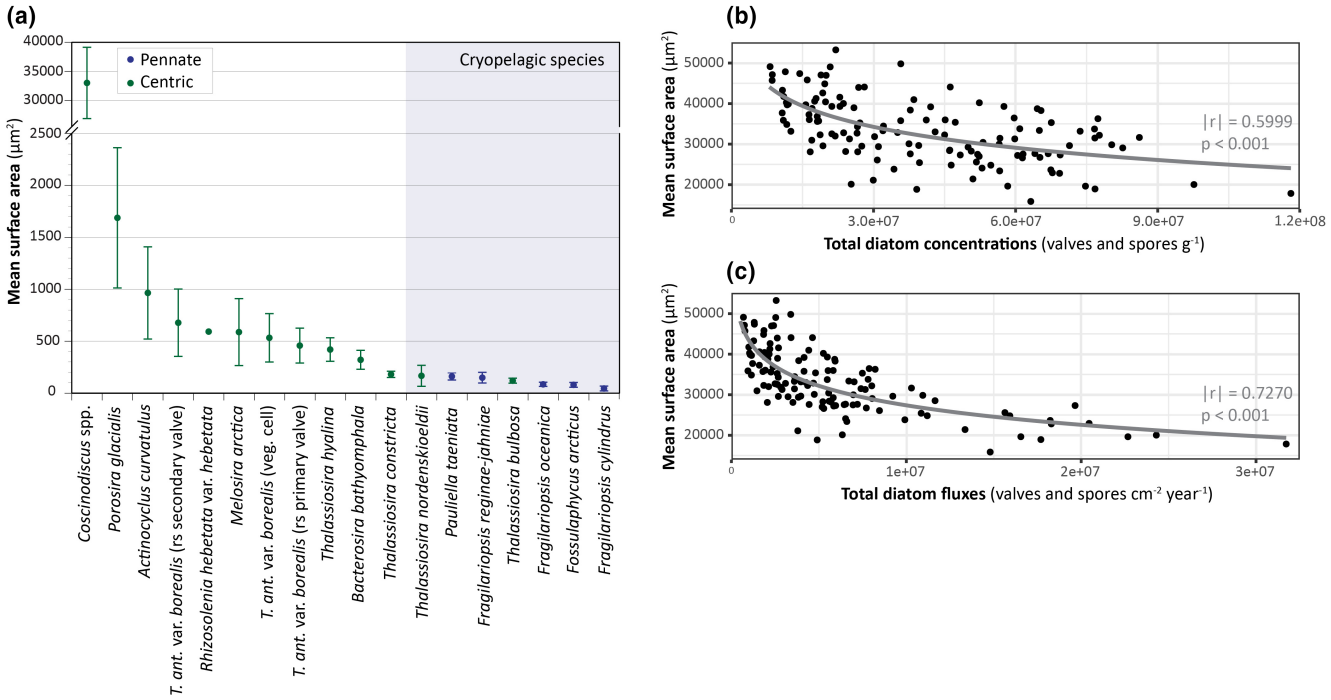


FIGURE 3 Diatom size. (a) Total mean surface area and SD ($\mu m^2$) of the main diatom taxa from core AMD15-Casq1, (b) moderate correlation between the mean surface area ($\mu m^2$) excluding *Coscinodiscus* spp. and total diatom concentration (valves $g^{-1}$; $|r| = .5999$; $y = -7438.7\ln(x) + 162{,}329.6$; $p < .001$), and (c) strong correlation between the mean surface area ($\mu m^2$) excluding *Coscinodiscus* spp. and total diatom fluxes (valves and spores·$cm^{-2}$·$year^{-1}$; $|r| = .7270$; $y = -6936.6\ln(x) + 139{,}189.4$; $p < .001$).

decline in June when *Chaetoceros* resting spores become important contributors to the sinking material, in response to nitrogen depletion (Michel et al., 2002; Tremblay et al., 2002). Rhizosolenids can exploit deeper sources of nutrients and thrive in stratified conditions and as such can contribute to the late succession stages (Kemp et al., 2000; Margalef, 1967).

## 5.1 | Regime shifts in the Pikialasorsuaq

Previous studies found that the NOW crossed an ecosystem regime shift at ca. 2000 cal years BP, at the transition to the Roman Warm Period (RWP; ca. 2000–1500 years BP; Wanner et al., 2008) and during an unprecedented strong positive phase of the Arctic Oscillation (Darby et al., 2012), which marked the beginning of an interval of polynya instability that lasted until ca. 800 years BP (Jackson et al., 2021; Ribeiro et al., 2021). An unstable Smith Sound ice arch allowed for increased export of sea ice from the Arctic Ocean into the NOW, was associated with a decline in marine primary production and little auk (*Alle alle*) colonies, and was coeval with an interval without evidence of human occupation in western Greenland (Ribeiro et al., 2021). Following Burgers et al. (2023), it is possible that the positive phase of the Arctic Oscillation may have been associated with enhanced contributions of fresher and nutrient-depleted waters from the Lincoln Sea into Nares Strait, exacerbating the unfavorable conditions for the biological productivity in the downstream NOW region. Jackson et al. (2021) also inferred an increased northward inflow of Atlantic water and less efficient brine production, especially during the RWP but also during the Medieval Climate Anomaly (MCA; ca. 1200–800 years BP), further pointing toward weaker/contracted polynya conditions during these warmer intervals of the Late Holocene.

The early part of our record, with the interval between ca. 2400 and 2050 cal years BP standing out in particular, suggests that the polynya generally maintained a relatively productive early spring bloom, based on high loading of the MIZ factor assemblage, high diatom concentrations and fluxes, and the marked presence of *T. bulbosa* and *T. hyalina* (Figure 2). However, from 2050 cal years BP, at the onset of the RWP, all four measures of diatom production changed significantly. Low diatom concentrations of about $10–20 \times 10^6$ valves per gram of dry sediment are comparable to those observed in nonpolynya settings such as offshore Upernavik (core AMD14-204) in northeastern Baffin Bay during the same period (Limoges et al., 2020). This marked decline in overall production was associated with an increase in the contribution of the Arctic and Arctic Greenland factor assemblages, suggesting a modification to the hydrographic properties with concurrent increases in the influence of both Arctic-sourced cold and fresh, as well as Atlantic-sourced, waters. Furthermore, a sudden shift to positive PC1 values was primarily steered by *Rhizosolenia* spp., *P. glacialis*, and the resting spores of *T. antarctica* var. *borealis*. *Rhizosolenia* spp. is associated with a more stratified water column, and *P. glacialis* has been reported from waters with high concentrations of slush and wave-exposed shore ice (Krebs et al., 1987). This is coherent with a change in the

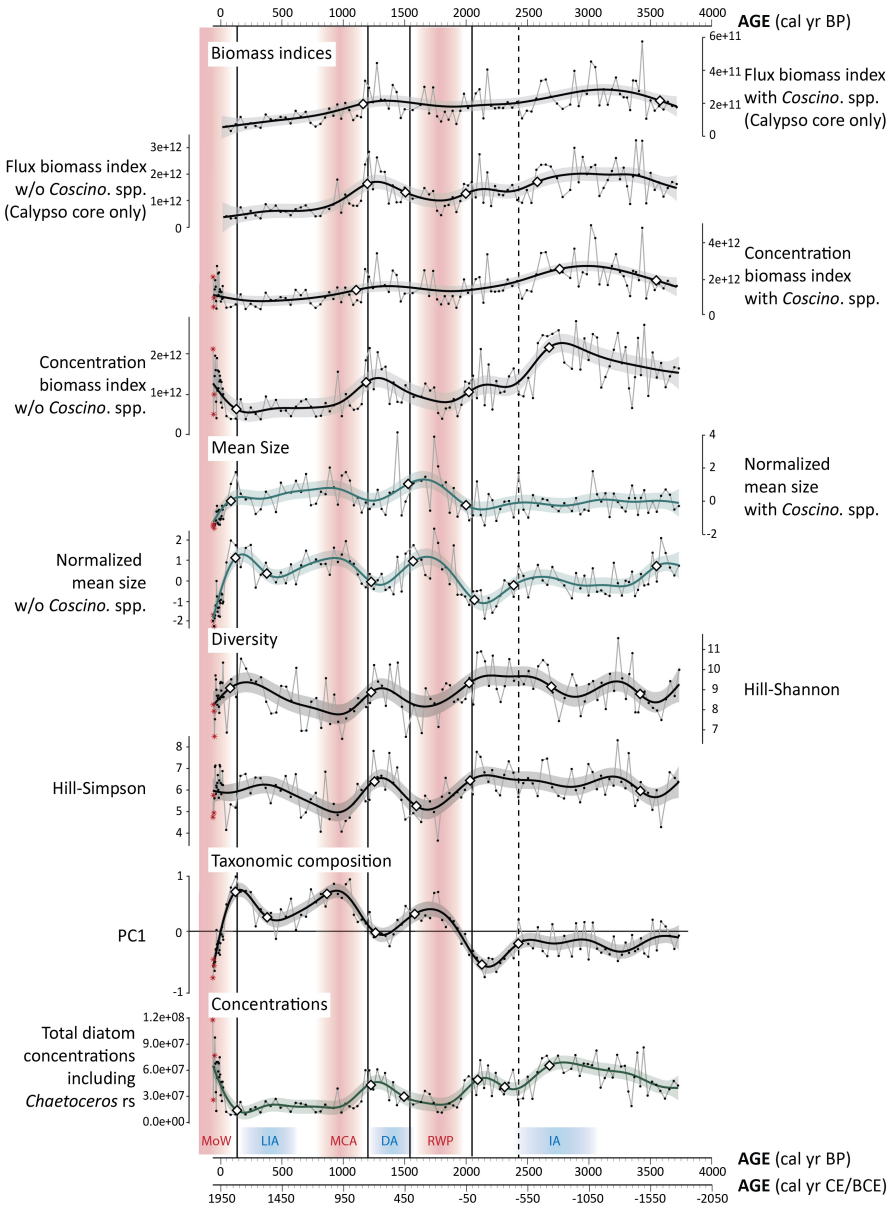


**FIGURE 4** Changes in the four main measures of export diatom production (total concentration, taxonomy, diversity, and mean size) and biomass indices over the last ca. 3800 years. Note that the flux biomass index was only calculated for the long Calypso core (see explanation in Section 4.1). For each parameter, the solid lines indicate the smoothed curve fitted by the GAM, and the light-colored areas represent the 95% confidence bands. The white diamonds indicate the start of significant change as identified from the first derivative of the GAM fit. The black vertical lines indicate times at which significant changes were identified in all four measures of diatom production (mean value; solid lines) and at least three measures of diatom production (dashed line). According to the age model, the recent interval (2007–2015 CE) of observed increased destabilization of the Nares Strait ice arch is recorded by the last three data points shown with red asterisks. DA, Dark Age; IA, Iron Age; LIA, Little Ice Age; MCA, Medieval Climate Anomaly; MoW, modern warming; RWP, Roman Warm Period.

oceanography of Kane Basin identified by Caron et al. (2019) from ca. 2100 cal years BP, with the potential collapse of the Smith Sound ice arch proposed by Georgiadis et al. (2020) and a much weaker or spatially reduced NOW at the onset of the RWP (Ribeiro et al., 2021) which would have facilitated the northward penetration of Atlantic-sourced water (Jackson et al., 2021). At a neighboring site (Site 012; Figure 1), Knudsen et al. (2008) noted the scarcity of diatoms during the same interval, with increased contribution of *Coscinodiscus* taxa. *Coscinodiscus* species, including *C. centralis* which is an important contributor to the NOW's diatom community (Lovejoy et al., 2002), are known to thrive at low-light irradiance levels under sea ice or at the base of the euphotic zone (Duerksen et al., 2014; Kemp et al., 2000). Therefore, our data clearly show that the critical environmental threshold identified in previous studies at the onset of the RWP not only translated into, and is coherent with, changes to the taxonomic composition of the diatom assemblages but furthermore that this regime shift was linked to a significant increase in mean diatom size and a decrease in diatom diversity (Figure 4; see also Section 5.2.).

Following these remarkable shifts, similar patterns are observed further up-core, with the warm MCA associated with decreased diatom concentration, increased mean size and decreased diversity (Figure 4), and the cold intervals of the Dark Ages (DA) and Little Ice Age (LIA) associated with decreased mean size and increased diversity and concentrations (summarized in Table 1). Very abrupt changes in diatom concentration, taxonomic composition, and mean size suggest that the NOW became stronger ca. 130 cal years BP (Figure 4), in contrast with the previous warmer intervals of the Late Holocene. For instance, whereas PC1 and mean size increased going into previous warmer intervals, these parameters show opposite patterns under the Modern Warming (MoW). Additionally, significant decreases in diatom concentration were recorded during previous warmer intervals, which contrasts with the marked increase in total diatom concentrations at

**TABLE 1** Summary of diatom community-level responses to changes in the Pikialasorsuaq during the Late Holocene and transition into the MoW.

| Intervals of the Late Holocene | Regime | Co-occurring environmental drivers | Community-level responses |
|---|---|---|---|
| IA, DA, LIA | Stable polynya | Cold(er) | ↑ Export production |
| | | Stable ice arch | ↓ PC1 scores |
| | | Low drift ice | ↑ Diversity |
| | | Mixed water column | ↓ Mean cell size |
| RWP, MCA | Weak/contracted polynya | Warm(er) | ↓ Export production |
| | | Ice arch instability/failure | ↑ PC1 scores |
| | | Drift ice | ↓ Diversity |
| | | Stratified water column | ↑ Mean cell size |
| Beginning MoW | Transitional state | Warm(er) | Large amplitude fluctuations export production |
| | | Increasing ice arch instability | ↓ PC1 scores |
| | | Increasing drift ice | ↓ Diversity |
| | | Increasing stratification | ↓ Mean cell size |

the beginning of the MoW, highlighting the different nature and boundary conditions of the latter (e.g., emerging from advanced Neoglacial cooling, timing based on instrumental observations vs. sedimentary and ice core records for previous warm intervals). While the observed destabilization of the southern Nares Strait ice arch of the 21st century is captured by the three last data points only which include just 3 years of ice arch failure between 2007 and 2015 CE, it is worth noting that these are characterized by a decrease in Hill–Shannon diversity and fluctuations in total diatom concentrations of an amplitude not seen elsewhere in the record, likely pointing to increasing instability. Overall, our results thus suggest that the system recently entered a new state that has no parallel in the last 3800 years BP.

## 5.2 | Significance of diatom community size structure and seasonality

From a macroevolutionary standpoint, it is still a matter of debate whether geometric characteristics are primarily driven by predation pressure or environmental conditions. In modern oceans, phytoplankton community size structure appears to be strongly shaped by physical processes of advection and turbulence and resulting nutrient availability in the euphotic zone (e.g., Cullen et al., 2002; Li, 2002; Margalef, 1978). Smaller cells with larger surface-to-volume ratios have faster growth rates and are commonly assumed to have a better ability to harvest nutrients and light, the latter resulting from their higher pigment-specific absorption efficiencies (Finkel et al., 2004). In sea-ice environments, the shallow spring water column stratification has therefore been interpreted to favor small cell sizes, which were thought to be better adapted to increase nutrient diffusion and reduce nutrient requirements and sinking rates (Finkel et al., 2009), whereas turbulent and nutrient-replete environments support larger cells. However, Behrenfeld et al. (2021) suggest that allometric scaling is associated with size-selective grazing pressure rather than physical constraints on nutrient uptake; for nutrient uptake, more important than the surface-to-volume ratio is the cytoplasmic volume served by a given area of the cell surface, which is weakly dependent on cell volume (Behrenfeld et al., 2008, 2021; Snoeijs et al., 2002). As such, the high division rates of thin and small bloom-forming species make that these can outpace losses from grazing, even when exerted by rapidly reproducing small predators, whereas the larger and slow-growing species are considered comparatively less palatable to grazers (Cullen et al., 2002). Prey–predator dynamics may therefore explain the seasonal successions upon alleviation of light limitation, with smaller species preceding larger species during the vernal blooms because of the tighter grazing control with decreasing size (Behrenfeld et al., 2021). As summarized by Acevedo-Trejos et al. (2018), size diversity is likely subject to trade-offs between nutrient uptake and the vulnerability to grazing.

Since we did not observe a major overturning in the composition of the fossil diatom communities throughout core AMD15-Casq1, it is unlikely that a secular pattern in the preservation of the small versus large-sized valves is responsible for the downcore variations in the size index. Instead, these variations are largely steered by the contribution of the small and fast-growing cryopelagic diatoms to the assemblages, notably *Fragilariopsis cylindrus/nana*, *F. oceanica* and *F. arcticus*. Today, the polynya offers an exceptionally high level of diatom production, at a critical time during the spring, opening an ecological niche for other organisms to succeed (e.g., Heide-Jørgensen et al., 2013). Many keystone species have adapted their life histories to this early source of abundant food. For example, the NOW supports the largest seabird populations in Greenland and these seabird colonies rely on the spring pulse of primary productivity (Davidson et al., 2018). In particular, sympagic and pelagic diatoms are the most important prey items for *Calanus* copepods (including *Calanus glacialis*; Søreide et al., 2008) on which little auks depend for foraging and raising their chicks (Davidson et al., 2018). Given the negative relationship between the size index

and the total diatom concentration/flux (Figure 3), we suggest that changes in the size index may reflect the amplitude and duration of the early spring bloom, with implications for the polynya's ecological function (e.g., flux of elements and flow of energy within food webs; Behrenfeld et al., 2021; Smetacek et al., 2004). Therefore, shifts in subfossil diatom community size structure can reveal alterations to the spring bloom phenology that likely affected the NOW ecosystem from the bottom up.

We calculated "biomass" indices to assess whether a change from numerically abundant small diatom species to less abundant but larger species compensated for the decrease in the total export diatom concentrations during the intervals of unstable ice arch/polynya conditions of the RWP and MCA. We found that even though the increased relative abundance of larger species may have contributed, to some extent, to ecosystem resilience during these intervals, the decline in the abundance of smaller taxa nonetheless had a dominant negative effect on total diatom biomass exported to the seafloor over the last 3800 years BP (Figures 4 and 5). This is underlined by the significant decline in the flux biomass index during both the RWP and MCA.

## 5.3 | Implications for the future

Since 1994 CE, the breakdown of the Nares Strait ice arch has taken place at the end of June, at least 2 weeks earlier than during the interval 1968–1994 CE (Blais et al., 2017). In years when the ice arch collapses even earlier (e.g., 2008 CE, end of May) or completely fails to form (2007, 2009, 2010, 2017, 2019, and 2022 CE), thick ice accumulates along the Canadian coast (Kwok et al., 2010; Moore et al., 2021; Vincent, 2020) while increased input of the fresh Arctic Ocean water and meltwater leads to a more stratified water column in the NOW (e.g., Blais et al., 2017; Figure 5). In this context, our results suggest that the predicted increased instability and earlier collapse of the Nares Strait ice arch for the coming decades will change the timing and taxonomic composition of seasonal phytoplankton successions and have the potential to dampen the production of small cryopelagic diatoms that are characteristic of the extended early spring bloom in the polynya. Our data further show that during the warm periods of the Late Holocene (RWP, MCA), shifts in the diatom community size structure to larger taxa that are more typical of the late(r) successional stages and subsurface conditions were associated with overall reduced export diatom production and diversity. Diatom productivity can furthermore be influenced by increased contributions of relatively nutrient-depleted water into Nares Strait during positive phases of the Arctic Oscillation (Burgers et al., 2023), as well as by feedback mechanisms such as those affecting global marine silica cycling (e.g., Taucher et al., 2022). Therefore, there remains a risk that changes in the diatom phenology will cascade through the food web, disproportionately impacting keystone species and subsistence resources that are critically important to global biodiversity and the communities from Inuit Nunangat and Greenland.

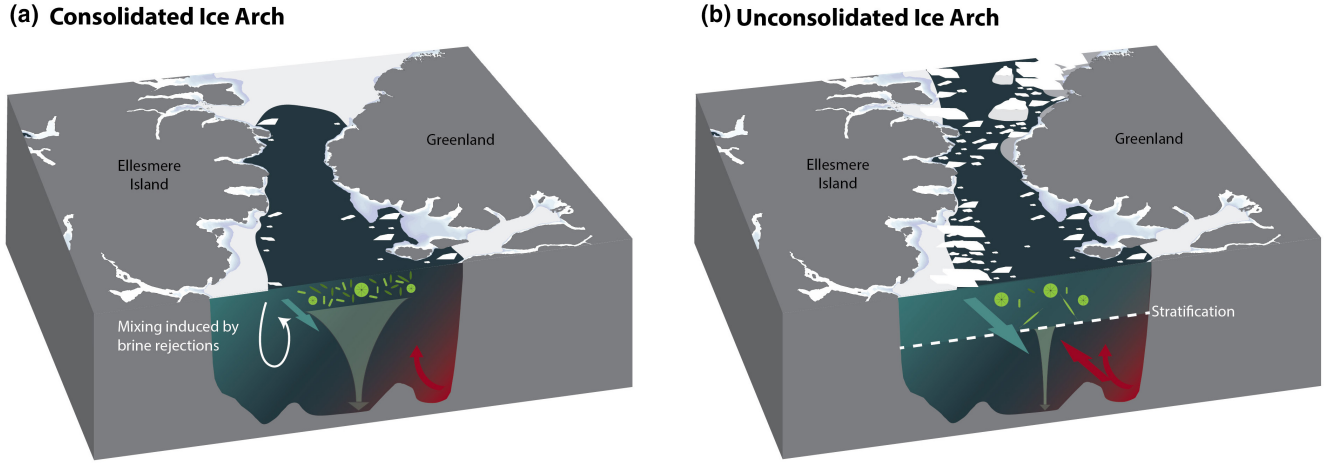


FIGURE 5 Schematic illustration of the Pikialasorsuaq during intervals of a spring (a) consolidated and (b) unconsolidated Smith Sound ice arch, illustrating the hypothesized contrasting stratification regimes. When the ice arch is present, a strong pulse of small fast-growing cryopelagic diatoms followed by pelagic diatoms contributes to high diatom export with higher taxonomic diversity to the seafloor. This pulsatile production of food is crucial to keystone species (e.g., seabirds including little auks) that have adapted their life history accordingly. By contrast, when the Smith Sound ice arch does not consolidate (b) such as inferred for the RWP (Georgiadis et al., 2020; Jackson et al., 2021; Ribeiro et al., 2021), and as projected for the future, increased ice floes, especially along the Ellesmere Island coast, and increased salinity stratification dampen diatom production. During the RWP, reduced brine production may have facilitated the northward penetration of the relatively warm water of the West Greenland Current (Jackson et al., 2021). Large diatom genera such as those typically associated with the late successional stages and subsurface conditions (e.g., *Rhizosolenia*) contribute more significantly to the export production, which is characterized by a lower taxonomic diversity.

## 6 | CONCLUSION

Understanding the phenology and functional structure of primary-producer communities in marine environments can improve our ability to project how climate-induced changes will affect ecosystems. In this study, Late Holocene export diatom production was described in terms of taxonomy, mean size, diversity, and total biomass. Our data suggest that diatom communities dominated by smaller taxa during strong polynya conditions of the Late Holocene accumulated more biomass and were more diverse than the communities dominated by larger cells during intervals of weaker/contracted polynya conditions of the RWP and MCA. While the Pikialasorsuaq has supported a highly productive ecosystem since the end of the LIA, high-amplitude fluctuations in total diatom concentrations and diversity decline during the 21st century may be the early signs of the polynya's increased instability. Further destabilization of the Nares Strait ice arch could lead to a transition into an "unconsolidated ice arch" productivity regime similar to that observed during the RWP, although high-amplitude fluctuations in diatom productivity and diversity changes in recent years may indicate that the NOW system is transitioning into a new state. Our results underline the importance of the small early spring cryopelagic diatoms for the functioning and productive capacity of the NOW ecosystem.

### AUTHOR CONTRIBUTIONS

Audrey Limoges, Kaarina Weckström, and Sofia Ribeiro conceptualized the study. Audrey Limoges performed the analyses and investigation with valuable taxonomic contributions from Kaarina Weckström and Xavier Crosta. Audrey Limoges, Nicolas Van Nieuwenhove, and Stephen Juggins performed statistical treatments. Rebecca Jackson provided updated age model data. Audrey Limoges wrote the manuscript and prepared the figures, and all the co-authors reviewed/edited the manuscript.

### ACKNOWLEDGMENTS

We thank the communities of Inuit Nunangat and Avernasuaq for allowing research in the Pikialasorsuaq region. We thank Guillaume Massé for his help during the initiation of this project. This study received financial support from the Natural Sciences and Engineering Research Council of Canada (NSERC; funding reference number 2018-03984) and ArcticNet (206) grants to A.L., Arctic Avenue (spearhead research project between the University of Helsinki and Stockholm University) to K.W., and the Independent Research Fund, Denmark (*Sapere Aude* grant 9064-00039B) to S.R. We thank Amundsen Science which is supported by the Canada Foundation for Innovation and NSERC. We thank officers, crew members, scientists, and chief scientist Philippe Archambault for their assistance in the collection of core AMD15-Casq1 during the ArcticNet 2015 Leg 4a onboard the Canadian research icebreaker CCGS Amundsen.

### CONFLICT OF INTEREST STATEMENT

The authors declare that they have no competing interests.

### DATA AVAILABILITY STATEMENT

The data that supports the findings of this study are available in supplementary material of this article and in Dryad at https://doi.org/10.5061/dryad.cz8w9gj8p.

### ORCID

*Audrey Limoges* https://orcid.org/0000-0002-4587-3417
*Kaarina Weckström* https://orcid.org/0000-0002-3889-0788

### REFERENCES

Acevedo-Trejos, E., Maranón, E., & Merico, A. (2018). Phytoplankton size diversity and ecosystem function relationships across oceanic regions. *Proceedings of the Royal Society B: Biological Sciences*, *285*, 1879. https://doi.org/10.1098/rspb.2018.0621

Barber, D. G., & Massom, R. A. (2007). Chapter 1 The role of sea ice in Arctic and Antarctic polynyas. *Elsevier Oceanography Series*, *74*, 1–54.

Behrenfeld, M. J., Halsey, K., & Milligan, A. (2008). Evolved physiological responses of phytoplankton to their integrated growth environment. *Philosophical Transactions of the Royal Society B: Biological Sciences*, *363*, 2687–2703.

Behrenfeld, M. J., Halsey, K. H., Boss, E., Karp-Boss, L., Milligan, A. J., & Peers, G. (2021). Thoughts on the evolution and ecological niche of diatoms. *Ecological Monographs*, *91*(3), e01457.

Blaauw, M., & Christen, J. A. (2011). Flexible paleoclimate age-depth models using an autoregressive gamma process. *Bayesian Analysis*, *6*(3), 457–474.

Blais, M., Ardyna, M., Gosselin, M., Dumont, D., Bélanger, S., Tremblay, J.-E., Gratton, Y., Marchese, C., & Poulin, M. (2017). Contrasting interannual changes in phytoplankton productivity and community structure in the coastal Canadian Arctic Ocean. *Limnology and Oceanography*, *62*(6), 2480–2497.

Brown, K. A., Holding, J. M., & Carmack, E. C. (2020). Understanding regional and seasonal variability is key to gaining a pan-Arctic perspective on Arctic Ocean freshening. *Frontiers in Marine Science*, *7*, 606.

Burgers, T. M., Miller, L. A., Rysgaard, S., Mortensen, J., Else, B., Tremblay, J.-É., & Papakyriakou, T. (2023). Distinguishing physical and biological controls on the carbon dynamics in a high-Arctic Outlet Strait. *Journal of Geophysical Research: Oceans*, *128*(3), e2022JC019393.

Caron, M., Rochon, A., Montero-Serrano, J.-C., & St-Onge, G. (2019). Evolution of sea-surface conditions on the northwestern Greenland margin during the Holocene. *Journal of Quaternary Science*, *34*, 1–12.

Coachman, L. K., & Aagaard, K. (1988). Physical oceanography of Arctic and subarctic seas. In T. Herman (Ed.), *Marine geology and oceanography of the Arctic seas*. Springer-Verlag.

Cornet-Barthaux, V., Armand, L., & Quéguiner, B. (2007). Biovolume and biomass estimates of key diatoms in the Southern Ocean. *Aquatic Microbial Ecology*, *48*, 295–308.

Crosta, X., & Koç, N. (2007). Diatoms: From micropaleontology to isotope geochemistry. In C. Hilaire-Marcel, & A. de Vernal (Eds.), *Proxies in Late Cenozoic Paleoceanography*, *Developments in Marine Geology Series* (Vol. *1*, pp. 327–369). Elsevier.

Crosta, X., Shukla, S. K., Ther, O., Ikehara, M., Yamane, M., & Yokoyama, Y. (2020). Last abundant appearance datum of *Hemidiscus karstenii* driven by climate change. *Marine Micropaleontology*, *157*, 101861.

Cullen, J. J., Franks, P. J. S., Karl, D. M., & Longhurst, A. (2002). Biological–physical interactions in the sea. In A. R. Robinson, J. J. McCarthy, & B. J. Rothschild (Eds.), *The Sea* (Vol. *12*, pp. 297–336). Wiley.

Dakos, V., Matthews, B., Hendry, A. P., Levine, J., Loeuille, N., Norberg, J., Nosil, P., Scheffer, M., & De Meester, L. (2019). Ecosystem tipping points in an evolving world. *Nature Ecology & Evolution*, *3*, 355–362.

Darby, D. A., Ortiz, J. D., Grosch, C. E., & Lund, S. P. (2012). 1,500-year cycle in the Arctic oscillation identified in Holocene Arctic Sea-ice drift. *Nature Geoscience*, *5*, 897–900.

Davidson, T. A., Wetterich, S., Johansen, K. L., Grønnow, B., Windirsch, T., Jeppesen, E., Syväranta, S., Olsen, J., González-Bergonzoni, I., Strunk, A., Larsen, N. K., Meyer, H., Søndergaard, J., Dietz, R., Eulears, I., & Mosbech, A. (2018). The history of seabird colonies and the North Water ecosystem: Contributions from paleoceological and archaeological evidence. *Ambio*, *47*, 175–192.

Duerksen, S. W., Thiemann, G. W., Budge, S. M., Poulin, M., Niemi, A., & Michel, C. (2014). Large, omega-3 rich, pelagic diatoms under arctic sea ice: Sources and implications for food webs. *PLoS One*, *9*(12), e114070.

Dumont, D., Gratton, Y., & Arbetter, T. E. (2010). Modeling wind-driven circulation and landfast ice-edge processes during polynya events in northern Baffin Bay. *American Meteorological Society*, *40*(6), 1356–1372.

Finkel, Z. V., Irwin, A., & Schofield, A. J. (2004). Resource limitation alters the ¾ size scaling of metabolic rates in phytoplankton. *Marine Ecological Progress Series*, *273*, 269–279.

Finkel, Z. V., Katz, M. E., Wright, J. D., Schofield, O. M. E., & Falkowski, P. (2005). Climatically driven macroevolutionary patterns in the size of marine diatoms over the Cenozoic. *Proceedings of the National Academy of Sciences of the United States of America*, *102*(25), 8927–8932.

Finkel, Z. V., Vaillancourt, C. J., Irwin, A. J., Reavie, E. D., & Smol, J. P. (2009). Environmental control of diatom community size structure varies across aquatic ecosystems. *Proceedings of the Royal Society B*, *276*, 1627–1634.

Georgiadis, E., Giraudeau, J., Jennings, A., Limoges, A., Jackson, R., Ribeiro, S., & Massé, G. (2020). Local and regional controls on Holocene Sea ice dynamics and oceanography in Nares Strait, Northwest Greenland. *Marine Geology*, *422*, 106115.

Hammer, Ø., Harper, D. A. T., & Ryan, P. D. (2001). PAST: Paleontological statistics software package for education and data analysis. *Palaeontologia Electronica*, *4*(1), *9*.

Heaton, T. J., Köhler, P., Butzin, M., Bard, E., Reimer, R. W., Austin, W. E. N., Ramsey, C. B., Grootes, P. M., Hughen, K. A., Kromer, B., Reimer, P. J., Adkins, J., Burke, A., Cook, M. S., Olsen, J., & Skinner, L. C. (2020). Marine20–The marine radiocarbon age calibration curve (0-55,000 cal BP). *Radiocarbon*, *62*, 779–820.

Heide-Jørgensen, M. P., Burt, L. M., Hansen, R. G., Nielsen, N. H., Rasmussen, M., Fossette, S., & Stern, H. (2013). The significance of the North Water polynya to Arctic top predators. *Ambio*, *42*(5), 596–610.

Hill, M. O. (1973). Diversity and evenness: A unifying notation and its consequences. *Ecology*, *54*, 427–432.

Hurd, D. C., & Birdwhistell, S. (1983). On producing a general model for biogenic silica dissolution. *American Journal of Science*, *283*, 1–28.

Imbrie, J., & Kipp, N. (1971). A new micropaleontological method for quantitative paeloclimatology: Application to a Late Pleistocene Caribbean core. In R. F. Flint (Ed.), *The late Cenozoic glacial ages* (pp. 71–181). Yale University Press.

Jackson, R., Kvoning, A. B., Limoges, A., Georgiadis, E., Olsen, S. M., Tallberg, P., Andersen, T. J., Mikkelsen, N., Giraudeau, J., Massé, G., Wacker, L., & Ribeiro, S. (2021). Holocene polynya dynamics and their interactions with oceanic heat transport in northernmost Baffin Bay. *Scientific Reports*, *11*, 10095.

Kamatani, A., & Riley, J. P. (1979). Rate of dissolution of diatom silica walls in seawater. *Marine Biology*, *55*, 29–35.

Kemp, A. E. S., Pike, J., Pearce, R. B., & Lange, C. B. (2000). The "fall dump"—A new perspective on the role of a "shade flora" in the annual cycle of diatom production and export flux. *Deep-Sea Research Part II*, *47*(9–11), 2129–2154.

Knudsen, K. L., Stabell, B., Seidenkrantz, M.-S., Eiríksson, J., & Blake, W. (2008). Deglacial and Holocene conditions in northernmost Baffin Bay: Sediments, foraminifera, diatoms and stable isotopes. *Boreas*, *37*, 346–376.

Koerner, K. A., Limoges, A., Van Nieuwenhove, N., Richerol, T., Massé, G., & Ribeiro, S. (2021). Late Holocene Sea-surface changes in the North Water polynya reveal freshening of northern Baffin Bay in the 21st century. *Global and Planetary Changes*, *206*, 103642.

Krebs, W. N., Lipps, J. H., & Burckle, L. H. (1987). Ice diatom floras, Arthur Harbor, Antarctica. *Polar Biology*, *7*, 163–171.

Kwok, R., Pedersen, L. T., Gudmandsen, P., & Pang, S. S. (2010). Large sea ice outflow into the Nares Strait in 2008. *Geophysical Research Letters*, *37*(3), L03502.

Lehmann, N., Kienast, M., Granger, J., & Tremblay, J.-É. (2022). Physical and biogeochemical influences of nutrients through the Canadian Arctic Archipelago: Insights from nitrate isotope ratios. *Journal of Geophysical Research: Oceans*, *127*, e2021JC018179.

Lewis, E. L., Ponton, D., Legendre, L., & LeBlanc, B. (1996). Springtime sensible heat, nutrients and phytoplankton in the North Water polynya, Canadian Arctic. *Continental Shelf Research*, *16*, 1775–1792.

Li, W. K. W. (2002). Macroecological patterns of phytoplankton in the northwestern North Atlantic Ocean. *Nature*, *419*, 154–157.

Limoges, A., Weckström, K., Ribeiro, S., Georgiadis, E., Hansen, K. E., Martinez, P., Seidenkrantz, M.-S., Martinez, P., Crosta, X., & Massé, G. (2020). Learning from the past: Impact of the Arctic oscillation on sea ice and marine productivity off Northwest Greenland over the last 9,000 years. *Global Change Biology*, *26*, 6767–6786.

Lovejoy, C., Legendre, L., Martineau, M.-J., Bâcle, J., & von Quillfeldt, C. H. (2002). Distribution of phytoplankton and other protists in the North Water. *Deep-Sea Research II*, *49*, 5027–5047.

Marchese, C., Albouy, C., Tremblay, J.-E., Dumont, D., D'Ortenzio, F., Vissault, S., & Bélanger, S. (2017). Changes in phytoplankton bloom phenology over the North Water (NOW) polynya: A response to changing environmental conditions. *Polar Biology*, *40*, 1721–1737.

Margalef, R. (1967). The food web in the pelagic environment. *Helgolander Wissenschaftliche Meeresuntersuchungen*, *15*(1–4), 548–559.

Margalef, R. (1978). Life forms of phytoplankton as survival alternatives in an unstable environment. *Oceanologica Acta*, *1*, 493–509.

McNeely, R., & Brennan, J. (2005). Geological survey of Canada revised shell dates. Open File 5019. https://doi.org/10.4095/221215

Melling, H., Graton, Y., & Ingram, G. (2001). Ocean circulation within the North Water polynya of Baffin Bay. *Atmosphere-Ocean*, *39*(3), 301–325. https://doi.org/10.1080/07055900.2001.9649683

Michel, C., Gosselin, M., & Nozais, C. (2002). Preferential sinking export of biogenic silica during the spring and summer in the North Water polynya (northern Baffin Bay): Temperature or biological control? *Journal of Geophysical Research*, *107*(C7), 1–14.

Michel, C., Hamilton, J., Hansen, E., Barber, D., Reigstad, M., Iacozza, J., Seuthe, L., & Niemi, A. (2015). Arctic Ocean outflow shelves in the changing Arctic: A review and perspectives. *Progress in Oceanography*, *139*, 66–88.

Möllmann, C., Folke, C., Edwards, M., & Conversi, A. (2015). Marine regime shifts around the globe: Theory, drivers and impacts. *Philosophical Transactions of the Royal Society of London. Series B: Biological Sciences*, *370*(1659), 20130260.

Moore, G. W. K., Howell, S. E. L., & Brady, M. (2023). Evolving relationship of Nares Strait ice arches on sea ice along the strait and the North Water, the Arctic's most productive polynya. *Scientific Reports*, *13*, 9809.

Moore, G. W. K., Howell, S. E. L., Brady, M., Xu, X., & McNail, K. (2021). Anomalous collapses of Nares Strait ice arches leads to enhanced export of Arctic Sea ice. *Nature Communications*, *12*, 1. https://doi.org/10.1038/s41467-020-20314-w

Mosbech, A., Johansen, K. L., Davidson, T., Appelt, M., Grønnow, B., Cuyler, C., Lyngs, P., & Flora, J. (2018). On the crucial importance of a small bird: The ecosystem services of the little auk (Alle alle) population in Northwest Greenland in a long-term perspective. *Ambio*, *47*, 226–243. https://doi.org/10.1007/s13280-018-1035-x

Münchow, A., Falkner, K., & Melling, H. (2007). Spatial continuity of measured seawater and tracer fluxes through Nares Strait, a dynamically wide channel bordering the Canadian Arctic archipelago. *Journal of Marine Research*, *65*(6), 759–788.

Münchow, A., Flakner, K., & Melling, H. (2015). Baffin Island and West Greenland current systems in northern Baffin Bay. *Progress in Oceanography*, *132*, 305–337.

Münchow, A., Melling, H., & Falkner, K. K. (2006). An observational estimate of volume and freshwater flux leaving the Arctic Ocean through Nares Strait. *Journal of Physical Oceanography*, *36*(11), 2025–2041.

Mundy, C. J., & Barber, D. G. (2001). On the relationship between spatial patterns of sea ice type and the mechanisms which create and maintain the North Water (NOW) polynya. *Atmosphere-Ocean*, *39*, 327–341.

Nelson, D. M., & Tréguer, P. (1992). Role of silicon as a limiting nutrient to Antarctic diatoms: Evidence from kinetics studies in the Ross Sea ice-edge zone. *Marine Ecology Progress Series*, *80*, 255–264.

Oksman, M., Juggins, S., Arto, M., Andrzej, W., & Weckström, K. (2019). The biogeography and ecology of common diatom species in the northern North Atlantic, and their implications for paleoceanographic reconstructions. *Marine Micropaleontology*, *148*, 1–28.

Oksman, M., Weckström, K., Miettinen, A., Juggins, S., Divine, D. V., Jackson, R., Telford, R., Korsgaard, N. J., & Kucera, M. (2017). Younger Dryas ice maring retreat triggered by ocean surface warming in central-eastern Baffin Bay. *Nature Communications*, *8*, 1017.

Pieńkowski, A., Coulthard, R. D., & Furze, M. F. A. (2023). Revised marine reservoir offset (ΔR) values for molluscs and marine mammals from Arctic North America. *Boreas*, *52*(2), 145–167.

Preußer, A., Heinemann, G., Willmes, S., & Paul, S. (2015). Multi-decadal variability of polynya characteristics and ice production in the North Water polynya by means of passive microwave and thermal infrared satellite imagery. *Remote Sensing*, *7*(12), 15807–15867.

R Core Team. (2022). *R: A language and environment for statistical computing*. R Foundation for Statistical Computing. https://www.R-project.org

Ragueneau, O., Tréguer, P., Leynaert, A., Anderson, R. F., Brzezinski, M. A., DeMaster, D. J., Dugdale, R. C., Dymond, J., Fischer, G., François, R., Heinze, C., Maier-Reimer, E., Martin-Jézéquel, V., Nelson, D. M., & Quéguiner, J. (2000). A review of the Si cycle in the modern ocean: Recent progress and missing gaps in the application of biogenic opal as a paleoproductivity proxy. *Global and Planetary Change*, *26*, 317–365.

Ren, H., Shokr, M., Li, X., Zhang, Z., Hui, F., & Cheng, X. (2022). Estimation of sea ice production in the North Water polynya based on ice arch duration in winter during 2006-2019. *JGR Oceans*, *127*(10), e2022JC018764.

Ribeiro, S., Limoges, A., Massé, G., Johansen, K. L., Colgan, W., Weckstrom, K., Jackson, R., Georgiadis, E., Mikkelsen, N., Kuijpers, A., Olsen, J., Olsen, S. M., Nissen, M., Andersen, T. J., Strunk, A., Wetterich, S., Syvaranta, J., Henderson, A. C. G., Mackay, H., … Davidson, T. A. (2021). Vulnerability of the North Water ecosystem to climate change. *Nature Communications*, *12*, 4475.

Roswell, M., Dushoff, J., & Winfree, R. (2021). A conceptual guide to measuring species diversity. *Oikos*, *130*, 321–338.

RStudio Team. (2022). *RStudio: Integrated development environment for R*. RStudio, PBC.

Ryabov, A., Kerimoglu, O., Litchman, E., Olenina, I., Roselli, L., Basset, A., Stanca, E., & Blasius, B. (2021). Shape matters: The relationship between cell geometry and diversity in phytoplankton. *Ecology Letters*, *24*(4), 847–861.

Simpson, G. L. (2018). Modelling palaeoecological time series using generalised additive models. *Frontiers in Ecology and Evolution*, *6*, 149. https://doi.org/10.3389/fevo.2018.00149

Simpson, G. L. (2022). gratia: Graceful ggplot-based graphics and other functions for GAMs fitted using mgcv. R package version 0.7.3 https://gavinsimpson.github.io/gratia

Smetacek, V., Assmy, P., & Henjes, J. (2004). The role of grazing in structuring Southern Ocean pelagic ecosystems and biogeochemical cycles. *Antarctic Science*, *16*, 541–558.

Snoeijs, P., Busse, S., & Potapova, M. (2002). The importance of diatom cell size in community analysis. *Journal of Phycology*, *38*, 265–272.

Søreide, J. E., Falk-Petersen, S., Hegseth, E. N., Hop, H., Carroll, M. L., Hobson, K. A., & Blachowiak-Samolyk, K. (2008). Seasonal feeding strategies of Calanus in the high-Arctic Svalbard region. *Deep Sea Research Part II: Topical Studies in Oceanography*, *55*(20–21), 2225–2244.

Steffen, K. (1985). Warm water cells in the North Water, northern Baffin Bay during winter. *Journal of Geophysical Research*, *90*, 9129–9136.

Taucher, J., Bach, L. T., Friederike Prowe, A. E., Boxhammer, T., Kvale, K., & Riebesell, U. (2022). Enhanced silica export in a future ocean triggers global diatom decline. *Nature*, *60*, 696–700.

Tréguer, P., Bowler, C., Moriceau, B., Dutkiewicz, S., Gehlen, M., Aumont, O., Bittner, L., Dugdale, R., Finkel, Z., Ludicone, D., Jahn, O., Guidi, L., Lasbleiz, M., Leblanc, K., Levy, M., & Pondaven, P. (2018). Influence of diatom diversity on the ocean biological carbon pump. *Nature Geoscience*, *11*, 27–37.

Tremblay, J.-E., Gratton, Y., Carmack, E. C., Payne, C. D., & Price, N. M. (2002). Impact of the large-scale Arctic circulation and the North Water polynya on nutrient inventories in Baffin Bay. *Journal of Geophysical Research*, *107*(C8), 26-1–26-14.

Tremblay, J. E., Hattori, H., Michel, C., Ringuette, M., Mei, Z.-P., Lovejoy, C., Fortier, L., Hobson, K. A., Amiel, D., & Cochran, J. K. (2006). Trophic structure and pathways of biogenic carbon flow in the eastern North Water polynya. *Progress in Oceanography*, *71*, 402–425.

Tremblay, J.-E., & Smith, W. O. (2007). Primary production and nutrient dynamics in polynyas. In W. O. Smith & D. G. Barber (Eds.), *Polynyas: Windows to the world* (pp. 239–269). Elsevier.

Vincent, R. F. (2019). A study of the North Water polynya ice arch using four decades of satellite data. *Scientific Reports*, *9*, 20278.

Vincent, R. F. (2020). An examination of the non-formation of the North Water polynya ice arch. *Remote Sensing*, *12*, 2712.

Vincent, R. F., & Marsden, R. F. (2008). A study of tidal influences in the North Water polynya using short time span satellite imagery. *Arctic*, *61*(4), 373–380.

Wanner, H., Beer, J., Bütikofer, J., Crowley, T. J., Cubasch, U., Flückiger, J., Goosse, H., Grosjean, M., Joos, F., Kaplan, J. O., Küttel, M., Müller, S. A., Prentice, I. C., Solomina, O., Stocker, T. F., Tarasov, P., Wagner, M., & Widmann, M. (2008). Mid- to Late Holocene climate change: An overview. *Quaternary Science Reviews*, *27*, 1791–1828.

Williams, K. M. (1986). Recent Arctic marine diatom assemblages from bottom sediments in Baffin Bay and Davis Strait. *Marine Micropaleontology*, *10*, 327–341.

Williams, K. M. (1990). Late Quaternary paleoceanography of the western Baffin Bay region evidence from fossil diatoms. *Canadian Journal of Earth Sciences*, *27*, 1487–1494.

Wood, S. N. (2017). *Generalized additive models: An introduction with R* (2nd ed.). Chapman and Hall/CRC. https://doi.org/10.1201/9781315370279

## SUPPORTING INFORMATION

Additional supporting information can be found online in the Supporting Information section at the end of this article.

**How to cite this article:** Limoges, A., Ribeiro, S., Van Nieuwenhove, N., Jackson, R., Juggins, S., Crosta, X., & Weckström, K. (2023). Marine diatoms record Late Holocene regime shifts in the Pikialasorsuaq ecosystem. *Global Change Biology*, *29*, 6503–6516. https://doi.org/10.1111/gcb.16958